Simulating pedestrian avoidance: The human-zombie game

Juan P. Oriana ●[*]

Instituto Tecnológico de Buenos Aires (ITBA), *Lavardén 315, 1437 C. A. de Buenos Aires, Argentina*

German A. Patterson ●[†] and Daniel R. Parisi ●[‡]

Instituto Tecnológico de Buenos Aires (ITBA), *CONICET*, *Lavardén 315, 1437 C. A. de Buenos Aires, Argentina*

This study introduces a simulated active matter system, applying the pedestrian collision avoidance paradigm, which involves dynamically adjusting the desired velocity. We present a human-zombie game set within a closed geometry, combining predator-prey behavior with a one-way contagion process that transforms prey into predators. The system demonstrates varied responses in our implemented model: with agents having the same maximum speeds, a single zombie always captures a human, whereas two zombies never capture a single human agent. As the number of human agents increases, observables such as the final fraction of zombie agents and total conversion times exhibit significant changes in the system's behavior at intermediate density values. Most notably, there is evidence of a first-order phase transition when analyzing the mean population speed as an order parameter.

I. INTRODUCTION

A fundamental aspect in pedestrian dynamics modeling [1,2] is describing how pedestrians navigate and avoid collisions in various environments. Initially, force-based models like the Social Force Model [3,4] and the Predictive Collision Avoidance Model [5] simulated collision avoidance maneuvers by applying elusive forces directly on the agents.

An alternative framework, as proposed by Wang *et al.* [6] and expanded in [7–9], involves dynamically adjusting the agents' desired velocity for navigation and avoidance. This method closely resembles natural walking behavior, wherein individuals adapt their speed and direction according to their surroundings, especially in scenarios where physical contact is absent. Moreover, this approach can be implemented in any microscopic agent model that has a specified target velocity, irrespective of whether the movement is defined by forces or rules.

Pedestrians typically avoid each other while walking under normal conditions; however, there are also more atypical yet interesting scenarios in which humans escape by running from a pursuing agent. An example is the globally recognized children's game "Tag," in which "it" chases others, attempting to tag them. Upon tagging, the roles change, with the "it" status passing to the tagged player. The game has many variants, some of which have evolved into sports, such as World Chase Tag [10] and Ultimate Kho Kho [11] in India.

A more perilous scenario is the running of the bulls, with the most famous event taking place in Pamplona (Spain) during the San Fermín Festival. In this scenario, bulls run on the streets alongside human runners who attempt not to be caught by the bulls [12]. The running of the bulls concludes at the bullring. Runners enter the bullring while the bulls are led away from it. Then, a harmless *vaquilla* (young cow) is released, initiating its pursuit of the people, and interesting swarm-like patterns emerge within the crowd in the circular arena [13,14].

In light of these real-world pedestrian pursuit scenarios, we propose a pedestrian-dynamics simulation game as a test bed for the previously mentioned collision avoidance framework, which involves dynamically adjusting the desired velocity of the modeled agent [6–9,15].

Our game represents a fictional system that imitates a predator-prey scenario. It involves agents resembling zombies (Z) attacking humans (H), drawing inspiration from prevalent depictions in popular culture such as movies, TV series, and novels [16–21].

Other fictional systems involving zombies have previously been explored as an analogy for understanding the transmission of infectious diseases [22–24]. These studies often consider macroscopic population variables governed by differential equations to model their dynamics. On the other hand, adopting a microscopic approach, Libál *et al.* [25] investigate an SCZR (Susceptible-Cleric-Zombie-Recovered) model by employing a population of self-propelled particles performing random motion.

In our proposed zombie-human system, particles exhibit movement directions determined by a specific heuristic. Zombie agents possess a desired velocity pointing toward the nearest human agent, while human agents aim to avoid zombies and collisions with walls and other humans. Additionally, our system is simplistic in terms of infection, following a SI (Susceptible-Infected) model. The agents have only

---
[*]Contact author: joriana@itba.edu.ar

[†]Contact author: gpatters@itba.edu.ar

[‡]Contact author: dparisi@itba.edu.ar

two states, and the only possible transition is unidirectional: $H \rightarrow Z$.

Beyond offering a distinctive and imaginative framework for the pedestrian navigation paradigm mentioned earlier, our proposed setting intriguingly amalgamates two concepts within a unified system: (1) predator-prey dynamics and (2) infectious disease contagion. This scenario stands out for its distinctive aspect: the contagion not only affects the prey but also transforms it into a predator.

Finally, it is worth mentioning that although parts of the proposed system are derived from real-world scenarios (such as running away from pursuers and collision avoidance mechanisms), other components (like the zombie contagion) are artificial. Therefore, the simulations should be understood as a mathematical game, in the sense of the game of life [26,27] or the minority game [28]. Additionally, we can frame the current study of simulated pedestrians within the broader context of active matter systems displaying complex behaviors, such as phase transitions [29–34].

II. GAME DEFINITION

The proposed human-zombie game includes the following components and rules:

(G1) A circular enclosure without doors.

(G2) Two types of agents: Humans (H) and Zombies (Z). Zombies will attempt to capture humans, while humans will try to escape.

(G3) The initial condition consists of one zombie agent at the center of the enclosure and N_h human agents randomly distributed, beyond a minimum distance from the zombie.

(G4) A pedestrian dynamics operational model.

(G5) A heuristic for zombies to pursue humans, and a heuristic for humans to avoid zombies, other humans, and obstacles.

(G6) An irreversible transformation process from human to zombie. Once a zombie touches a human agent, both will remain stationary at this position for a certain period of time.

In the following subsections, models G4 and G5 are described, and parameter values are specified in Sec. III.

A. Operational model

Both types of agents share the operational model, which encompasses the basic mechanisms of motion through space and reactions upon contact and at high densities. We selected the rule-based Contractile Particle Model (CPM), demonstrated to reproduce experimental values for specific flows through doors and the fundamental diagram in unidirectional flow [35].

The CPM is a first-order model in which the position of particle i ($\mathbf{x}_i$) is updated following

$$\mathbf{x}_i(t + \Delta t) = \mathbf{x}_i(t) + \mathbf{v}_i \Delta t, \tag{1}$$

where $\mathbf{v}_i$ is the velocity and Δt is the simulation time step.

The direction and sense of the velocity are given by the unit vector $\mathbf{e}_i^0 = \frac{\mathbf{x}_i^0 - \mathbf{x}_i}{|\mathbf{x}_i^0 - \mathbf{x}_i|}$, where $\mathbf{x}_i^0$ is a target point fixed in space that must be chosen manually depending on the desired configuration to be simulated, in the same way as many other operational models such as the Social Force Model [4].
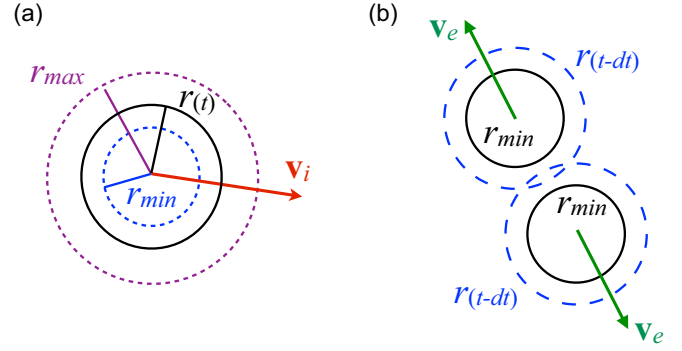

FIG. 1. Schematic representation of the operational Contractile Particle Model [35]. (a) A single free particle traveling with its current radius, bounded between $r_{\min}$ and $r_{\max}$, at its corresponding speed [Eq. (2)]. (b) When the radii of two particles come into contact, they both collapse to $r_{\min}$ and escape velocities are generated for one time step to separate the particles.

The magnitude of the velocity (v_i) is given as a function of the radius r_i, as

$$|\mathbf{v}_i| = v_i = v_i^{\max} \left(\frac{r_i - r_{\min}}{r_{\max} - r_{\min}} \right)^{\beta}, \tag{2}$$

where β is a constant. This unique property of having a variable radius within the range from $r_{\min}$ to $r_{\max}$ gives the name to the CPM. The agent's maximum velocity $v^{\max}$ is the free velocity.

In the case particle i is not in contact with any other particle or obstacle [see Fig. 1(a)], the radius increases according to Eq. (3) until the maximum radius is reached ($r_i = r_{\max}$):

$$r_i(t + \Delta t) = \min \left[r_{\max}, r_i(t) + \frac{r_{\max}}{\tau / \Delta t} \right], \tag{3}$$

where τ is a characteristic time constant giving the duration it takes for a particle to reach its maximum speed after starting from rest.

On the other hand, when particle radii overlap, the state of the involved particles is updated as follows: They contract their radii to the minimum value, $r_{\min}$, and for only one time step, their velocities assume the values $\mathbf{v}_e$ in a direction determined by the center of the two particles, each moving away from the other. The magnitude of this escape-from-contact velocity corresponds to the maximum velocity, $v_e = v^{\max}$. An illustration of this process can be seen in Fig. 1(b).

In our specific scenario, the interaction between humans and zombies results in the immobilization of both agents for a period t_c, representing the contagion process. Upon completion, the human agent transforms into a zombie and emerges with a radius of $r = r_{\min}$.

Additionally, to counteract artifacts arising from symmetric configurations, we add a small angular noise to the direction of the desired velocity following the model of self-propelled particles proposed by Vicsek et al. [30]. Let θ_i represent the angle formed by $\mathbf{v}_i$ with respect to the positive x semiaxis, and let θ_i^t denote the angle of the desired direction vector of agent i, thus, $\theta_i = \theta_i^t + \Delta\theta$, with $\Delta\theta$ defined as a uniform random value within the range of $[-\mu/2, \mu/2]$.
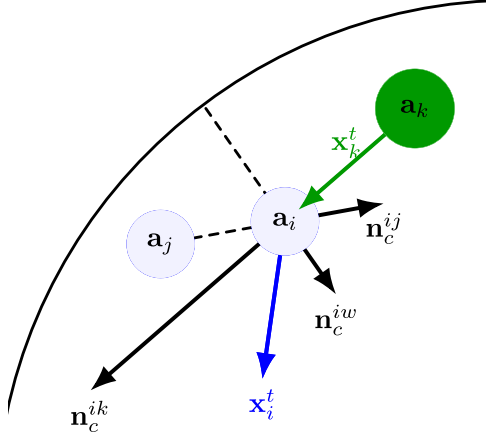
FIG. 2. Selection of the dynamic target $\mathbf{x}_i^t$ for a human agent a_i depends on the positions of the wall, another human a_j, and a zombie agent a_k. Also depicted the dynamic target $\mathbf{x}_k^t$ for a zombie agent a_k, solely dependent on human agent a_i.

B. Pursuit and evasion heuristics

A navigation layer can be implemented on top of the CPM by dynamically adjusting the direction of the velocity while agent i is not in contact with others. To achieve this, we replace the fixed target denoted by $\mathbf{x}_i^0$ in Sec. II A by a target that evolves with time $\mathbf{x}_i^t$, and thus the velocity reads $\mathbf{v}_i = v_i \mathbf{e}_i^t$, where the unit vector is $\mathbf{e}_i^t = \frac{\mathbf{x}_i^t - \mathbf{x}_i}{|\mathbf{x}_i^t - \mathbf{x}_i|}$. The heuristic for defining $\mathbf{x}_i^t$ varies depending on the agent type.

If agent k is a zombie, its target is the position of the nearest human agent h, defined by $\mathbf{x}_k^t = \mathbf{x}_h$, as illustrated for the (green) k particle in Fig. 2. This approach ensures that each zombie will continuously pursue the nearest human agent over time. Zombie agents will not attempt to avoid collisions, but will instead move directly towards the nearest human.

In the case where agent i is a human, $\mathbf{x}_i^t$ is obtained from the sum of the collision vectors $\mathbf{n}_c^{ij}$, which can be seen schematically in Fig. 2. Each $\mathbf{n}_c^{ij}$ quantifies the extent to which human i should adjust its direction to move away from agent j. Therefore, this desired target is defined by

$$\mathbf{x}_i^t = \sum_{z \in Z^i} \mathbf{n}_c^{iz} + \sum_{h \in H^i} \mathbf{n}_c^{ih} + \mathbf{n}_c^{iw}, \tag{4}$$

where the variables z and h iterate over zombie and human agents, respectively, Z^i represents the set of the N_z^e nearest zombies to agent i, and H^i denotes the set of the N_h^e nearest humans to agent i.

The vectors $\mathbf{n}_c^{ij}$ are computed as

$$\mathbf{n}_c^{ij} = \mathbf{e}^{ij} A e^{-\frac{d_{ij}}{B}}, \tag{5}$$

where d_{ij} is the distance between agents, $\mathbf{e}^{ij} = \frac{\mathbf{x}^i - \mathbf{x}^j}{|\mathbf{x}^i - \mathbf{x}^j|}$ is the direction from agent j to agent i, and A and B are constants denoting the intensity and a characteristic length, respectively. The last term, $\mathbf{n}_c^{iw}$, accounts for the interaction of agent i with walls. The point $\mathbf{x}^w$ is defined as the nearest point on the boundary to agent i.
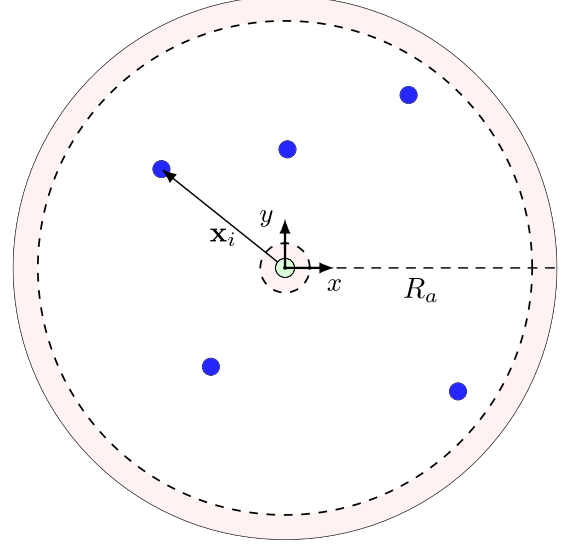

FIG. 3. Illustration of the simulation domain and the initial configuration featuring one zombie agent at the center (green, light gray) and $N_h = 5$ human agents (blue, dark gray).

III. SIMULATIONS

The agents move within a circular arena with a radius $R_a = 11$ m, as shown in Fig. 3. The simulations begin with only one zombie agent positioned at the center of the domain, and $N_h(t = 0) \equiv N_h$ human agents randomly distributed, ensuring that their distance from both the center and the wall exceeds 1 m (1 m $\leqslant |\mathbf{x}_i| \leqslant R_a - 1$ m), as illustrated by the dotted circles in Fig. 3.

Considering the model described in Secs. II A and II B, the parameters that do not depend on the types of agents are $\Delta t = 0.05$ s; $r_{\min} = 0.15$ m; $r_{\max} = 0.35$ m; $\beta = 0.9$; $\tau = 0.5$ s; $\mu = 0.052$ rad (3°); and $t_c = 3$ s. The parameters that differ depending on the type of agent are $A_h = 4$; $B_h = 1$ m; $N_h^e = 1$; $A_z = 8$; $B_z = 4$ m; $N_z^e = 2$; $A_w = 8$; and $B_w = 1$ m. Note that the intensity and range of a human agent avoiding a zombie are greater than those for avoiding another human agent.

Additionally, the free speed is different depending on the type of agent:

$$v_i^{\max} = \begin{cases} v_z^{\max} & \text{if agent } i \text{ is a zombie,} \\ v_h^{\max} & \text{if agent } i \text{ is a human.} \end{cases} \tag{6}$$

The specific values used in the simulations are $v_h^{\max} = 4.0$ m/s and $v_z^{\max} \in [3.8, 4.2]$ m/s, in steps of 0.1 m/s.

The initial number of humans (N_h) will vary between 10 and 100, in steps of five, and is considered the control parameter. It is important to note that the total number of agents is $N = N_h + 1$ (N_h humans plus one zombie), and this number remains constant in each simulation as human agents turn into zombies. Overall, considering the five values of the maximum zombie speed, there are a total of 95 system configurations to explore. The statistical analysis of each was conducted on 2500 realizations of random initial conditions. Each realization continued until either all agents had become zombies or the simulated time reached $t_{\max} = 2000$ s. We define the final

simulation time as T, and the number of simulation steps as S. Hence, $S = \frac{T}{\Delta t}$. In the case that $T = t_{\max}$, then $S = 40\,000$.

We will now define the observables under investigation. First, the fraction of zombies at any given time t in a realization k is given by

$$\phi_z^k(t) = \frac{N_z^k(t)}{N_h^k + 1} = \frac{N_z^k(t)}{N} \qquad (7)$$

and we compute $\langle \phi_z(t) \rangle$, which represents the average of ϕ_z^k across the realizations. We focus our study on the endpoint of the average final zombie fraction (hereafter referred to simply as the final zombie fraction), denoted as $\langle \phi_z^{\text{final}} \rangle$, which is defined when $\langle \phi_z(t) \rangle$ reaches a stationary value.

The second observable we calculate is the time required to achieve total conversion, denoted as the "total conversion time," T_c, and we average it across all realizations as the "average total conversion time," $\langle T_c \rangle$. Any realization that did not achieve total conversion within $t_{\max}$ was excluded from this particular analysis. If fewer than 10% of realizations achieve total conversion, that specific configuration will not be considered for analysis.

The last observable we define is the mean velocity, used as a type of order parameter. This is based on the understanding that zombie-human interactions typically occur at zero velocity, consequently reducing the mean velocity of the agents. This reduction is even more significant than the usual decrease caused by density in pedestrian dynamics and the CPM model [35].

Considering a specific realization k at time t, the system's velocity, accounting for both agent types, is expressed as follows:

$$v^k(t) = \frac{1}{N} \sum_{i=1}^{N} |\mathbf{v}_i^k(t)|, \qquad (8)$$

where $\mathbf{v}_i$ is the vector velocity of particle i. Then we compute the average across the realizations as

$$\bar{v} = \bar{v}(t) = \frac{1}{K} \sum_{k=1}^{K} v^k(t), \qquad (9)$$

with $K = 2500$, the number of realizations per configuration. Lastly, in the case of stationary states, the time average of mean population velocity is computed as $\langle \bar{v} \rangle_t$.

IV. RESULTS

A. Dynamics involving two and three agents

The behaviors of the system when $N_h = 1$ and $N_h = 2$ are interesting and notably different from one another. In the simplest scenario, the system consists of a single human agent ($N_h = 1$) in addition to the initial zombie [$N_z(t = 0) = 1$] within the simulation domain. We will show that, under conditions of equal maximum speed ($v_z^{\max} = v_h^{\max} = v^{\max}$), the zombie will always catch the human agent.

In the long-term pursuit between a human agent and a zombie, the human's trajectory becomes circular, running parallel to the enclosure's wall. This behavior is illustrated in Fig. 4(a), showing the trajectories of both agents. Figure 4(b) depicts the distance between this agents over time. The zombie agent
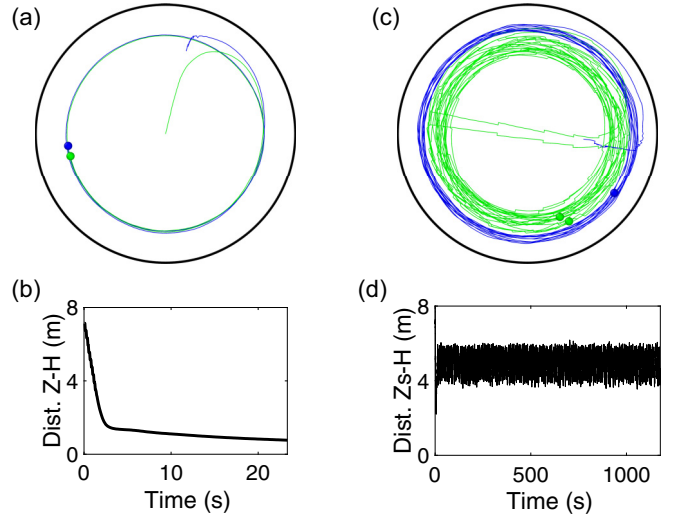

FIG. 4. Dynamics with two and three agents. (a) Trajectories of a zombie agent pursuing one human agent. (b) Evolution of the distance between these two agents. (c) Trajectories of two zombie agents (after the first conversion in the $N_h = 2$ case) pursuing one human agent. (d) Evolution of the distance between the center of mass of the two zombies and the human agent.

pursues the prey with a smaller turning radius, resulting in a higher angular velocity. Consequently, the zombie always catches up with its prey. See the Supplemental Material [14] for a video showing this dynamics.

This outcome indicates that in our simulations, when the speed of zombies is similar to that of humans, the initial zombie will inevitably succeed in converting at least one human. This claim is strengthened by the fact that human agents must evade not just walls, but also other agents, which, on top of that, can reduce their speed.

An important consideration is the potential for a human to escape if a model incorporating inertia and the capability for zig-zag evasive maneuvers is employed. Under these conditions, the aforementioned conclusion regarding an isolated human escaping from a zombie would no longer hold.

Let us now examine the immediately more intricate case ($N_h = 2$), showcasing behavior markedly distinct from the $N_h = 1$ scenario. Under this condition, the zombie chases the nearest human until it catches it, which will definitely happen, as demonstrated above. After converting the human into a zombie, the system's state changes to $N_z(t) = 2$ and $N_h(t) = 1$. Given these conditions, with both zombies having only one remaining human target, they both move towards that individual. With the two zombies being in close proximity following the conversion, they collide while moving towards the same target (as defined in Sec. II B, the heuristic for zombie agents does not result in avoidance between them). Such trajectories can be observed in Fig. 4(c). This collision decelerates the zombies, granting the human an opportunity to run away from both of them at maximum speed. As they resume their approach towards the target, after a few time steps, they collide once more, again diminishing their speed and allowing the human to distance themselves again. This pattern repeats indefinitely, ensuring that two zombies, both with maximum desired speeds equal to that of the human, can

never catch it, within the context of this operational model. The evolution of the distance between the center of mass of the two zombie agents and the human, fluctuating in the range of 4–6 m, is plotted in Fig. 4(d), and an animation of this dynamics can be viewed in the Supplemental Material [14].

Summing up, under the given conditions, when $N_h = 1$ the conversion will always be complete, i.e., $\phi_z = 1$. In contrast, this will never occur when $N_h = 2$, resulting in a stable zombie fraction of $\phi_z = 2/3$.

It is worth mentioning that this peculiar behavior of the system is due, at least in part, to two model idealizations. First, the heuristic for zombie agents compels them to move towards humans regardless of obstacles, in line with zombie behavior depicted in movies; they do not avoid contact with anything. Their mutual collisions result in the CPM model slowing down the agents' speeds when their radii come into contact. This rule of the CPM effectively reproduces the pedestrian fundamental diagram under unidirectional normal flow conditions [35], and it is somewhat reasonable to assume that two runners at a short distance would interfere with each other's movements [12]. Second, and perhaps more importantly, the zombie agents have exactly the same speed and start pursuing from a very similar location where the conversion took place. Introducing a dispersion in the zombies' speed could change the observed behavior.

B. Dynamics involving more than three agents

Having previously analyzed the fundamental cases of one and two humans, we now turn our attention to more densely populated initial conditions.

To illustrate the system's dynamics, we present several representative snapshots in Fig. 5 for different initial values of N_h, taken at specific moments corresponding to distinct zombie fractions.

It is crucial to highlight that after the first conversion (when reaching $N_z = 2$), the two zombies may either target the same human agent or different ones, depending on the positions of other human agents. In the former scenario, a loop could arise where the remaining humans can escape from the two zombies that continuously collide with each other (similar to the $N_h = 2$ scenario discussed in the previous Sec. IV A). This scenario is termed "convergent pursuit," and a video example is available in the Supplemental Material [14]. In the latter scenario, where the two zombies split to pursue different human agents, they will succeed, mirroring the $N_h = 1$ situation described in Sec. IV A. This is referred to as "divergent pursuit," and a video is available in the Supplemental Material [14]. Additionally, snapshots of both types of pursuit can be seen in Fig. 5(b) for "divergent" and Figs. 5(e) and 5(h) for "convergent."

After establishing these definitions, simulations are categorized based on the following criteria: if, after the initial conversion, both zombies remain within a distance of less than 2 m for 3 sec, the scenario is classified as convergent pursuit. Otherwise, it falls under divergent pursuit.

Figure 6 shows that the distribution of total simulations between each category is fairly balanced. However, when considering only simulations that result in total conversion, the only mechanism leading to total conversion for $N_h \leqslant 25$
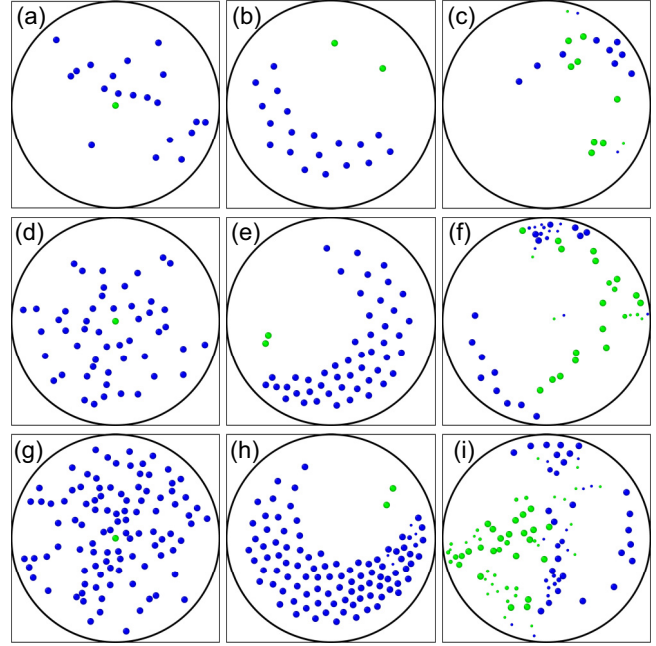

FIG. 5. Temporal evolution of three exemplary configurations. Panels (a), (d), and (g) show the initial conditions with a single zombie agent (green, light gray) at the center, for $N_h = 20, 50$, and 100, respectively. Panels (b), (e), and (h) display snapshots after the first conversion, for the same values of N_h. Panels (c), (f), and (i) depict the system when half of the initial humans have been converted ($\phi_z = 0.5$), for the same three values of N_h.

is the divergent pursuit type. As N_h increases, a transition is observed, reaching a balance after $N_h \geqslant 45$. In this region of elevated densities, both types of initial pursuits exhibit comparable probabilities of achieving total conversion due to the decelerating effect caused by the increased density of human agents.
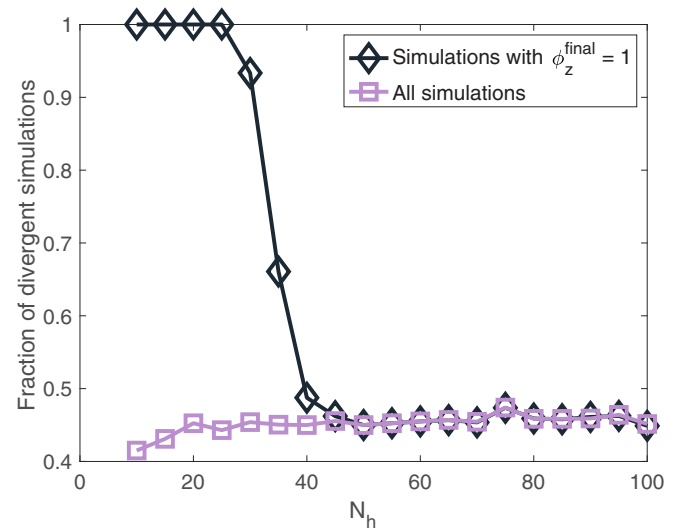

FIG. 6. Fraction of divergent pursuit cases as a function of the number of initial human agents in the system with a maximum zombie speed of $v_z^{\max} = v_h^{\max} = 4$ m/s.
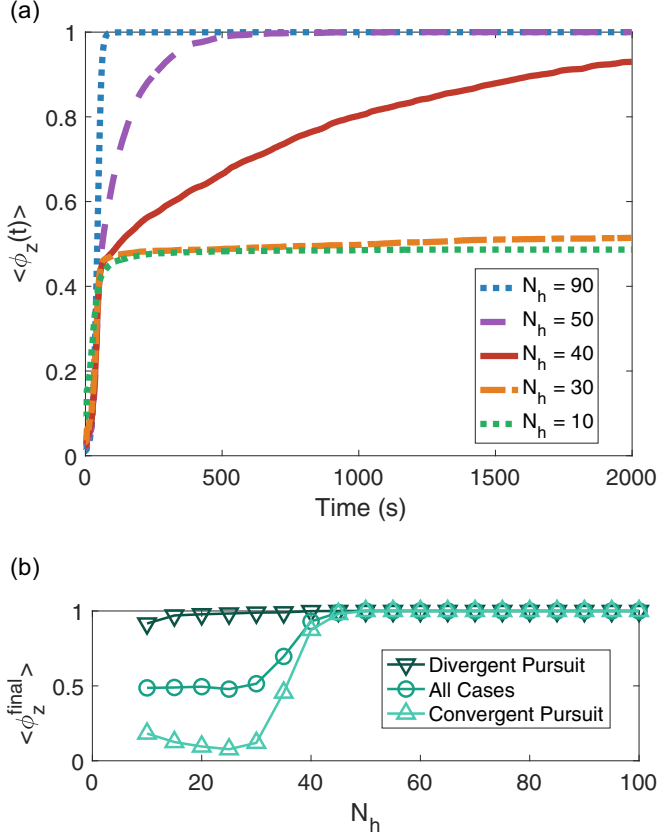
FIG. 7. Zombie fraction. (a) Time evolution of ϕ_z for $v_z^{\max} = 4$ m/s and the specified N_h values. (The order of the curves is the same as the order in the legend.) (b) Final zombie fraction ϕ_z^{final} as a function of the initial number of human agents, categorized by the type of pursuit.

In the following subsections, we further characterize the system's behavior, using the initial human density as the primary control parameter.

1. Final zombie fraction

In this section we examine the dynamics of the population, focusing on the average final zombie fraction, $\langle \phi_z^{\text{final}} \rangle$ [Eq. (7)]. Since the number of agents remains constant in each simulation, the fraction of human agents is complementary to the zombie fraction:

$\langle \phi_z^{\text{final}} \rangle = 1 - \langle \phi_h^{\text{final}} \rangle$. Consequently, we focus our discussion solely on the zombie fraction.

First, we examine the time evolution of $\langle \phi_z(t) \rangle$ in Fig. 7(a) for the scenario where $v_z^{\max} = v_h^{\max} = 4$ m/s. The mean zombie fraction is observed to reach stationary values within the simulation time, clustering around low and high values of N_h. A notable transition occurs around intermediate values of $N_h \sim 40$, requiring more time to reach the stationary regime.

This transition becomes clearer in Fig. 7(b), where $\langle \phi_z^{\text{final}} \rangle$ is plotted against the initial number of human agents. The curve labeled "All cases" represents the stationary data points from Fig. 7(a). For values up to $N_h = 30$, the final zombie fraction is $\langle \phi_z^{\text{final}} \rangle \approx 0.5$. However, beyond $N_h = 45$, the system invariably results in total conversion.
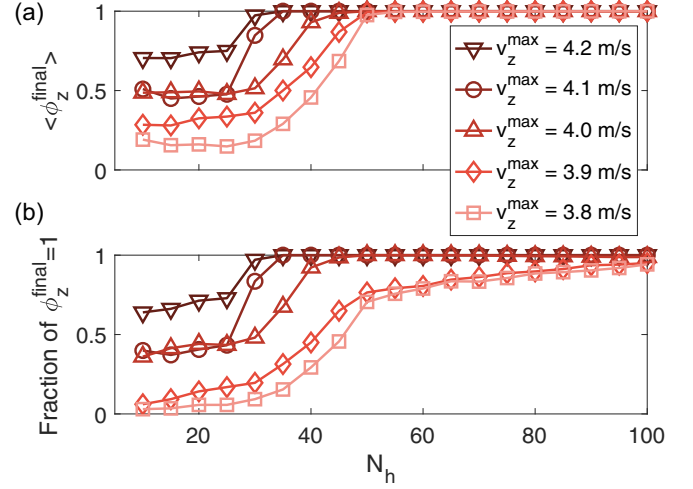

FIG. 8. Final conversion for $v_z^{\max}$ lower and higher than $v_h^{\max}$. (a) Final zombie fraction as a function of N_h for various $v_z^{\max}$ values. (The order of the curves is the same as the order in the legend.) (b) Ratio of realizations resulting in total conversion to the total number of simulations conducted for each N_h and $v_z^{\max}$ value.

The intermediate values of $\langle \phi_z^{\text{final}} \rangle$ at lower N_h arise from two extreme possible outcomes of the simulations: one with a very high zombie fraction and the other with a very low one. In the latter scenario, humans have ample space to outpace the zombies, who collide with each other, impeding their pursuit (convergent pursuit). Figure 7(b) illustrates that these two extremes correspond to divergent and convergent pursuit scenarios. This confirms our earlier observations from the analysis of Fig. 6: total conversion at lower N_h values is solely observed in cases of divergent pursuit. A counterintuitive behavior is observed in the case of convergent pursuit for low N_h values. The decrease in $\langle \phi_z^{\text{final}} \rangle$ between $N_h \in [10, 25]$ occurs because, in this range, there is enough space for human agents to not interfere with each other. Consequently, after the first conversion, which results in $N_z = 2$, these convergent zombies cannot reach any of the remaining humans, regardless of whether there are 10 or 25. Thus, the fraction of zombies, $\phi_z^{\text{final}} = 2/25$, is lower than $\phi_z^{\text{final}} = 2/10$.

On the other hand, when the initial human population exceeds $N_h \sim 45$, the constrained space inhibits human escape without mutual interference. This heightened density reduces their speed, invariably leading to zombies catching them, regardless of pursuit type.

Now we explore the same observable for varying maximum zombie speeds, maintaining a constant human maximum speed of $v_h^{\max} = 4$ m/s. Figure 8(a) displays five curves corresponding to $v_z^{\max} \in [3.8, 4.2]$ m/s. Observations reveal that the curves qualitatively exhibit a similar pattern, showing a transition from partial to total conversion at intermediate N_h values. However, as $v_z^{\max}$ increases, the final zombie fraction at lower N_h values decreases, and the N_h value at which the system saturates becomes higher. Both observations support the concept that higher-speed zombies can capture all human agents at lower critical densities. Additionally, the likelihood of converting the entire population becomes higher at these lower densities.
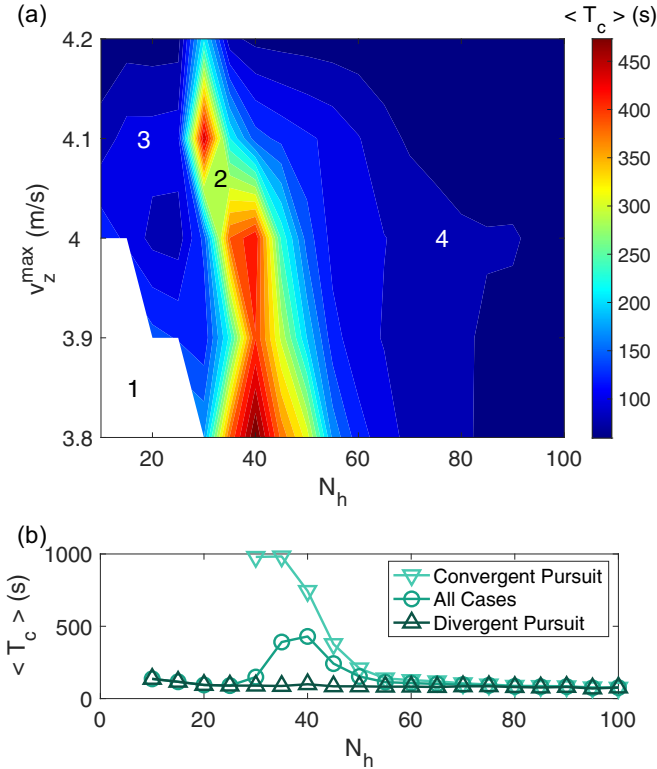
FIG. 9. Average total conversion time. (a) Phase diagram in the space v_z^{max}-N_h. (b) For the case $v_z^{max} = v_h^{max} = 4$ m/s, discriminated by the type of pursuit.

In Fig. 8(b) the fraction of simulations achieving total conversion is shown. For the cases of $v_z^{max} \geqslant v_h^{max} = 4$ m/s, the trend mirrors that of the final zombie fraction, albeit with noticeable differences observed for lower values of v_z^{max}. This occurs because a small portion of the realizations fail to achieve total conversion. This is primarily caused by multiple zombies colliding among themselves while pursuing a single human agent, preventing them from catching it. Furthermore, in instances where total conversion does not occur, the final fraction tends to be significantly high, usually around $\phi_z \sim \frac{N_h}{N_h+1}$. This explains the disparities between Figs. 8(a) and 8(b) when the maximum zombie speed is lower than the human speed. The video of a specific realization for this scenario is available in the Supplemental Material [14], with $v_z^{max} = 3.8$ m/s being less than v_h^{max}.

A particular case of conversion occurs when the entire population is converted, meaning $\phi_z = 1$. For the subset of simulations in which this happens, the relevant observable is the time needed for total conversion, and this analysis is presented in the next subsection.

2. Total conversion times

Total conversion is not always attained, being more probable at higher values of N_h and v_z^{max} as Fig. 8(b) clearly shows. Hence, the pertinent simulations within this context constitute a subset of those discussed in the preceding section. With this in mind, Fig. 9(a) illustrates the average total conversion time as a function of the initial number of human agents and the maximum zombie speeds. Intriguingly, a maximum

is observed for all zombie speeds, although this maximum is lower in the case of $v_z^{max} = 4.2$ m/s. In scenarios where zombie speeds exceed human speed, the peak conversion time occurs near $N_h \sim 30$, while for zombie speeds lower than or equal to human speed, the peak is around $N_h \sim 40$.

This suggests that achieving complete contagion occurs relatively quickly, irrespective of whether the initial number of humans is small or large. With fewer humans, they are less easily captured, yet the total conversion time remains low due to the smaller count of agents requiring conversion. Conversely, scenarios with a high number of humans result in easier capture (as density reduces their speed). At intermediate human numbers, a balance between these effects emerges: they are not easily captured, yet their adequate numbers contribute to slowing down the process.

Additional insight is presented in Fig. 9(b), where scenarios of convergent and divergent pursuit are delineated for the case of zombie speed equal to human speed ($v_z^{max} = v_h^{max}$). Convergent pursuit results in total conversion only for $N_h \geqslant 30$, and, as expected, it represents a slow process that results in prolonged conversion times for intermediate values of N_h. In contrast, divergent pursuit serves as the sole mechanism for achieving total conversion at lower N_h values, occurring more rapidly. The peak observed in total conversion times distinctly arises from averaging the swift conversions in divergent pursuit with the slower, diminishing conversion times linked to convergent pursuit.

Figure 9(a) depicts a phase diagram in which four regions can be identified. Region 1 (white) indicates the parameter region where total conversion cannot be attained ($< T_c > \to \infty$). Region 2 (red) is a mountain range where conversion times are maximum for all explored maximum zombie speeds, and it acts as a border between (blue) regions 3 and 4. Region 3 represents low conversion times due solely to divergent pursuit because convergent pursuit does not achieve total conversion at these low human densities. Finally, region 4 also indicates low conversion times, but due to high human agent densities which impede their escape from being captured by zombie agents at both low and high maximum zombie speeds.

Regarding both the conversion fraction analyzed in Sec. IV B 1 and the total conversion times discussed in this section, a change in system behavior is observed at intermediate values of initial human agent density. To characterize these behavioral changes in more detail, we will examine the system's average velocities in the following section.

3. Mean population velocities

Previous studies have suggested a shift in the system's behavior at intermediate N_h values. To delve deeper into this phenomenon, we will now investigate the system's mean speed.

The determination of mean velocity becomes less straightforward when humans and zombies possess different maximum speeds. In cases where $v_z^{max} < v_h^{max}$, the mean speed at low N_h takes an indefinitely long time to stabilize. Conversely, in scenarios where $v_z^{max} > v_h^{max}$, simulations with high N_h values typically result in total conversions before the mean speed can stabilize.
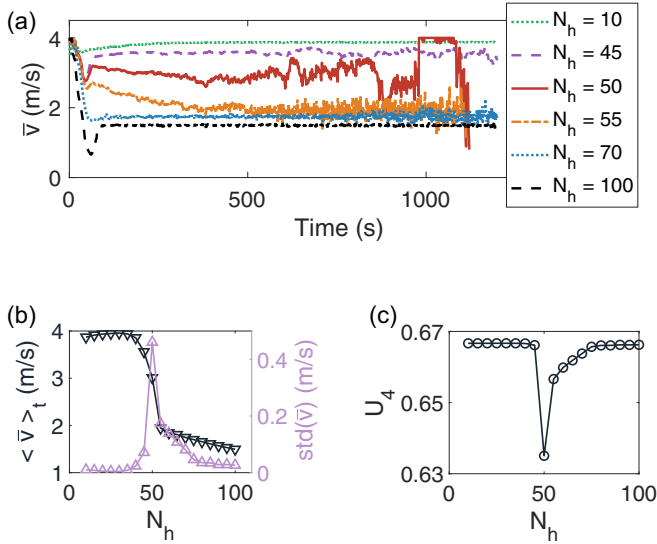
FIG. 10. Population velocities for the scenario $v_z^{max} = v_h^{max} = 4$ m/s with various N_h values. (a) Evolution of population velocity averaged across all realizations. (The order of the curves in the range 100–500 s is the same as the order in the legend.) (b) Mean population velocities after $t = 250$ s, accompanied by the corresponding standard deviation. (c) Binder parameter computed using the same data as in panel (b).

Stationary mean population speeds are evident solely when humans and zombies share equal maximum speeds ($v_z^{max} = v_h^{max}$), as depicted in Fig. 10(a). This figure also demonstrates that the stationary speed for low N_h is close to the maximum ($\bar{v} \approx v_z^{max} \approx v_h^{max} \approx 4$ m/s), while for high N_h, the mean speed falls below 2 m/s. At intermediate N_h values, there is a noticeable transition in mean speed between these two groups.

This transition becomes clearer when examining the temporal mean in the stationary regime of mean speed (considered after $t = 250$ s), as shown in Fig. 10(b). The standard deviations of the mean speed peak at $N_h = 50$, suggesting a potential phase transition at the critical value $N_{hc} \approx 50$. In Fig. 10(c) the fourth-order Binder cumulant $U_4 = 1 - \frac{\langle \bar{v}^4 \rangle_t}{3\langle \bar{v}^2 \rangle_t^2}$ is computed for the same data, exhibiting a distinct minimum at N_{hc}, indicative of a first-order transition [36].

V. CONCLUSIONS AND FUTURE DIRECTIONS

Employing an operational model of pedestrian dynamics [35], known for replicating the decrease in average speeds with increasing density (fundamental diagram of pedestrian traffic), we enhanced it by integrating evasion and pursuit mechanisms based on the agent's type. Prey agents (humans) transition to the predator state (zombies) upon capture by the predator.

This system not only acts as a test scenario for implementing the collision avoidance paradigm, where alterations are made solely to the agents' desired velocity, but it also exhibits a nontrivial emergent dynamic.

In basic scenarios involving two or three agents, it was observed that within a confined space, a predator can consistently catch its prey, even when they possess identical maximum speeds. However, when two predators pursue the same prey, their interference diminishes their speed, preventing them from ever capturing the sole prey.

The mutual collision mechanism can be disrupted when multiple preys exist, and each predator pursues a different prey. This scenario, termed "divergent pursuit," becomes a crucial factor in achieving total conversion in environments characterized by lower population density.

In scenarios involving numerous agents, we regard the global density (N_h, the initial number of humans) as the control parameter. Both the final zombie fraction and the average times for total conversion manifest a distinct behavioral change at intermediate N_h values. In the case of the final zombie fraction, it abruptly transitions from $\phi_z^{final} = 0.5$ to $\phi_z^{final} = 1$, and for the total conversion times, a peak is observed at values of N_h that depend on the maximum zombie speed.

Remarkably, when considering the average population velocity as an order parameter in scenarios where the maximum speeds of humans and zombies are equal, the results present evidence of a first-order phase transition occurring at the critical value of $N_{hc} \approx 50$.

The proposed human-zombie scenario could be expanded into more complex versions by including several probabilistic elements: the chance that a human can eliminate a zombie, the likelihood of a human being immune, and the possibility of a zombie being cured and reverting to a human state. These additions would introduce new dynamics and complexities to the system.

Regarding the possibility of implementing an experimental version of the theoretical game proposed, we can consider one of the many variants of the game "Tag" known as "Infection Tag," "Virus Tag," or "Zombie Tag." At the beginning of the game, there is only one zombie, which can multiply by tagging humans, turning them into zombies. This game could be aligned with our model by matching the "Zombie Tag" rules with those defined in Sec. II. Components G1–G3 can be implemented straightforwardly. Components G4 and G5 will be replaced by the real movement, avoidance, and pursuit mechanisms of people. This would imply a significant difference from our theoretical game, as people acting as "zombies" will avoid collisions. Rule G6 can easily be added, using the conversion time to reverse the side of a visible marker, like a bicolored cap or a T-shirt, to indicate the state of the players to others.

[1] A. Schadschneider, W. Klingsch, H. Klüpfel, T. Kretz, C. Rogsch, and A. Seyfried, in *Encyclopedia of Complexity and Systems Science*, edited by R. A. Meyers (Springer, New York, 2009), pp. 3142–3176.

[2] A. Corbetta and F. Toschi, Annu. Rev. Condens. Matter Phys. **14**, 311 (2023).

[3] D. Helbing and P. Molnár, Phys. Rev. E **51**, 4282 (1995).

[4] D. Helbing, I. Farkas, and T. Vicsek, Nature (London) **407**, 487 (2000).

[5] I. Karamouzas, P. Heil, P. Van Beek, and M. H. Overmars, in *Motion in Games: Second International Workshop, MIG 2009, Zeist, the Netherlands, November 21–24, 2009, Proceedings 2*, edited by A. Egges, R. Geraerts, and M. Overmars (Springer, Berlin, Heidelberg, 2009), pp. 41–52.

[6] Q.-L. Wang, Y. Chen, H.-R. Dong, M. Zhou, and B. Ning, Chin. Phys. B **24**, 038901 (2015).

[7] R. Martin and D. Parisi, Collective Dynamics **5**, 324 (2020).

[8] R. F. Martin and D. R. Parisi, in *Traffic and Granular Flow 2019*, edited by I. Zuriguel, A. Garcimartin, and R. Cruz (Springer International Publishing, Cham, 2020), pp. 205–210.

[9] R. F. Martin and D. R. Parisi, Physica A Stat. Mech. Appl. **633**, 129414 (2024).

[10] https://www.worldchasetag.com/about

[11] https://www.ultimatekhokho.com/.

[12] D. R. Parisi, A. G. Sartorio, J. R. Colonnello, A. Garcimartín, L. A. Pugnaloni, and I. Zuriguel, Proc. Natl. Acad. Sci. USA **118**, e2107827118 (2021).

[13] https://www.youtube.com/watch?v=07fb-2fwB5c

[14] See Supplemental Material at http://link.aps.org/supplemental/10.1103/PhysRevE.110.024611 for an illustration of the typical process of a young cow pursuing runners as well as videos showing the dynamics of one initial human agent, two initial human agents, the dynamics of convergent pursuit, the dynamics of divergent pursuit, and the typical dynamics when $v_z^{\max} = 3.8$ m/s and $v_h^{\max} = 4$ m/s.

[15] R. F. Martin and D. R. Parisi, Neurocomputing **379**, 130 (2020).

[16] Night of the Living Dead (1968, George A. Romero), https://www.imdb.com/title/tt0063350.

[17] Zombieland (2009, Ruben Fleischer), https://www.imdb.com/title/tt1156398.

[18] World War Z (2013, Marc Forster), https://www.imdb.com/title/tt0816711.

[19] Train to Busan (2016, Yeon Sang-Ho), https://www.imdb.com/title/tt5700672.

[20] Black Summer (2019, TV series), https://www.imdb.com/title/tt8923854.

[21] M. Brooks, *The Zombie Survival Guide: Complete Protection from the Living Dead* (Crown, New York, 2003).

[22] P. Munz, I. Hudea, J. Imad, and R. J. Smith, Infect. Dis. Model. Res. Prog. **4**, 133 (2009).

[23] A. A. Alemi, M. Bierbaum, C. R. Myers, and J. P. Sethna, Phys. Rev. E **92**, 052801 (2015).

[24] H. Bauer, Undergraduate thesis, University of Lynchburg, 2019.

[25] A. Libál, P. Forgács, Á. Néda, C. Reichhardt, N. Hengartner, and C. J. O. Reichhardt, Phys. Rev. E **107**, 024604 (2023).

[26] M. Gardner, Sci. Am. **223**, 210 (1970).

[27] M. Gardner, Sci. Am. **224**, 112 (1971).

[28] D. Challet and Y.-C. Zhang, Physica A **246**, 407 (1997).

[29] A. Syed, S. P. Thampi, and M. V. Panchagnula, Physica A **598**, 127349 (2022).

[30] T. Vicsek, A. Czirók, E. Ben-Jacob, I. Cohen, and O. Shochet, Phys. Rev. Lett. **75**, 1226 (1995).

[31] J. T. Siebert, F. Dittrich, F. Schmid, K. Binder, T. Speck, and P. Virnau, Phys. Rev. E **98**, 030601(R) (2018).

[32] M. Aldana, V. Dossetti, C. Huepe, V. M. Kenkre, and H. Larralde, Phys. Rev. Lett. **98**, 095702 (2007).

[33] G. Baglietto and E. V. Albano, Phys. Rev. E **78**, 021125 (2008).

[34] E. Barone and G. A. Patterson, Phys. Rev. E **109**, 054609 (2024).

[35] G. Baglietto and D. R. Parisi, Phys. Rev. E **83**, 056117 (2011).

[36] M. L. R. Puzzo, E. S. Loscar, A. De Virgiliis, and T. S. Grigera, J. Phys.: Condens. Matter **34**, 314001 (2022).